Semiconductors

DOI: 10.1002/anie.200503172

Transition-Metal Doped Zinc Oxide Nanowires**

*Benjamin D. Yuhas, David O. Zitoun, Peter J. Pauzauskie, Rongrui He, and Peidong Yang**

The introduction of impurity atoms into semiconducting materials is the primary method for controlling the properties of the semiconductor, such as band gap or electrical conductivity. This practice is routinely performed with bulk semiconductors and, more recently, has been extended to nanoscale semiconductors as well. In particular, II–VI and III–V semiconductors that have been doped with transition metals are currently generating much research interest, principally for their novel magnetic properties. These semiconductors are commonly called dilute magnetic semiconductors and are envisioned to be potential building blocks for spintronic devices.

One such material is transition-metal doped zinc oxide ($Zn_{1-x}M_xO$), which has been theoretically predicted to be ferromagnetic at room temperature.[1,2] Although this system has been under experimental study for some time, the vast majority of research conducted on this material has been done on bulk crystals or thin films.[3–8] There are very few reports on the fabrication of one-dimensional nanostructures of $Zn_{1-x}M_xO$, and high-temperature, vapor-phase methods are employed in the syntheses.[9,10] Although this approach has proven quite effective for the production of a multitude of nanoscale semiconductors, gas-phase syntheses are considerably limited in regards to homogeneous doping and alloying because of high-growth temperatures.

Solution-based synthetic schemes possess inherent advantages in the above areas over vapor-phase routes, in addition to ecological benefits. Whereas there have been several reports on the synthesis of pure ZnO nanowires from the solution phase,[11–13] the only solution-based methods for the production of $Zn_{1-x}M_xO$ yield isotropic quantum dots, such as those reported by Gamelin et al.[14,15] To date, no reports of anisotropic, transition-metal doped ZnO nanowires grown from the solution phase exist. We present herein the synthesis and characterization of cobalt-doped zinc oxide ($Zn_{1-x}Co_xO$) nanowires grown by a solution-phase synthesis. The synthetic process presented herein also allows for the doping of different transition metals (e.g., Mn, Fe, Cu); however, this report is limited to the cobalt-doped system.

The nanowires were synthesized by the thermal decomposition of zinc acetate and cobalt(II) acetate in refluxing trioctylamine (see the Experimental Section). Figure 1 shows scanning electron microscopy (SEM) and transmission electron microscopy (TEM) images of both pure and Co-doped ZnO nanowires. The nanowires grow in bundles that are tethered to a common hexagonal base. The diameter of the nanowires is statistically invariant regardless of the cobalt concentration. The average nanowire diameter is approximately 35 nm; the wires, thus, have aspect ratios that range from 80–160.

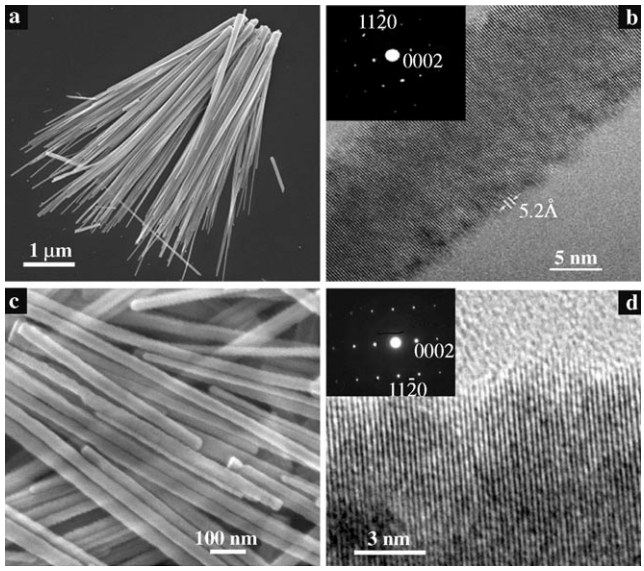

Figure 1. a) SEM image of undoped ZnO nanowires. b) High-resolution TEM image of a single ZnO nanowire, with an accompanying electron-diffraction pattern in the inset; similar images for Co-doped ZnO nanowires are shown in (c and d), in which Co content = 11.34%.

From the TEM images and selected-area electron-diffraction patterns (inset, Figure 1b, d), it is seen that the wires are single-crystalline, with a growth direction along the [0001] axis. This one-dimensional growth of pure ZnO nanowires has been reported previously in aqueous solutions.[11,12] In those examples, the one-dimensional growth was enabled by the presence of an amine moiety; we believe that the trioctylamine solvent plays a similar role in our system. It should also be noted that we observed similar single-crystalline diffraction patterns whether we examined a single wire or its base, thus indicating that the base likely nucleates first, followed by individual nanowire growth in the [0001] direction.

[*] B. D. Yuhas, Dr. D. O. Zitoun,[+] P. J. Pauzauskie, R. He, Prof. P. Yang
Department of Chemistry
Lawrence Berkeley National Laboratory
University of California
Berkeley, CA 94720 (USA)
E-mail: p_yang@berkeley.edu

[+] Current Address: LAMMI bat. 15
Université Montpellier II
Place Eugene Bataillon
34095 Montpellier Cedex 5 (France)

[**] This work was supported by the US Department of Energy. D.O.Z. is a DGA post-doctoral fellow. We thank Tevye Kuykendall and Josh Goldberger for their assistance in transmission electron microscopy (TEM) imaging. We thank Yulia Pushkar and Vittal Yachandra for their experimental assistance with electron paramagnetic resonance (EPR). P.J.P. thanks the NSF for a graduate research fellowship. Work at the Lawrence Berkeley National Laboratory was supported by the Office of Science, Basic Energy Sciences, Division of Materials Science, US Department of Energy. We thank the National Center for Electron Microscopy for the use of their facilities.

The cobalt concentration in the nanowires was determined by energy-dispersive X-ray (EDX) spectroscopy. The cobalt concentration (in atom%) can be varied from less than 1% to greater than 15% depending on the amount of cobalt precursor used; the most heavily doped sample in this investigation had a cobalt concentration of 11.34%. The cobalt amounts between different bundles of wires, as well as along individual wires, are very consistent; we saw a homogeneous concentration of cobalt in our samples and no evidence of a lateral or longitudinal concentration gradient in individual wires. Also, no indication of cobalt metal or cobalt oxide impurities in our final product was observed. Powder X-ray diffraction patterns of nanowires with various levels of cobalt doping are presented in Figure 2. In all cases, wurtzite

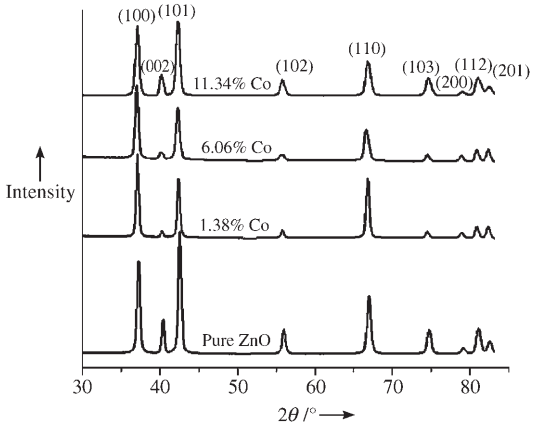

Figure 2. Powder X-ray diffraction patterns of pure and Co-doped ZnO nanowires.

is the only phase in existence, which indicates that doping is uniform throughout the nanowires. No significant shift in the lattice constants of the nanowires was seen either, although the cobalt and zinc ionic radii are so similar ($Zn^{2+} \approx 0.60$ Å, $Co^{2+} \approx 0.56$ Å) that any expected shift in lattice constant would be beyond the resolution of our diffractometer.

Electron energy-loss spectroscopy (EELS) was employed to determine the oxidation state of the cobalt in the wurtzite lattice. Figure 3 shows the EELS spectra obtained from the doped nanowires and three cobalt-containing standards. It is

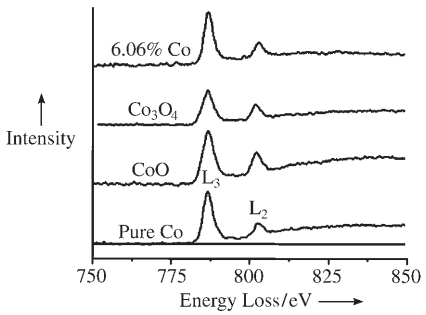

Sample	L_3/L_2 Area Ratio
6.06% Co	2.93
Pure Co	3.77
CoO	2.90
Co_3O_4	2.43

Figure 3. EELS spectra of 6.06% Co-doped ZnO Nanowires and cobalt-containing standards.

known that the L_3 and L_2 EELS peaks of the first-transition-series elements are sensitive to the oxidation state of the metal.[16,17] By comparing the areas of the L_3 and L_2 peaks in the EELS spectra, the oxidation state of the cobalt in the nanowires can be determined. The table in Figure 3 lists the resulting area ratios, and it can be seen that the nanowires correlate very well with the ratio obtained from CoO, a divalent cobalt compound, thus indicating that cobalt exists in a divalent state (Co^{2+}) in the ZnO host semiconductor.

The nanowires are of excellent optical quality, as shown by a series of photoluminescence (PL) measurements (Figure 4). When excited with ultraviolet light, the pure ZnO nanowires exhibit band-edge luminescence near 380 nm, accompanied by a broad defect band centered at approximately 550 nm. Both of the above peaks diminish in intensity upon cobalt inclusion, and a new peak centered at 680 nm appears. This wavelength corresponds well with the $^4T_1(P) \rightarrow {}^4A_2(F)$ transition that is indicative of a Co^{2+} ion in a tetrahedral crystal field,[18–21] and this transition is visible in all of our doped-nanowire samples.

The single peak at 680 nm splits into several separate components at low temperature, and this splitting is reproducible from sample to sample. It is known from previous electronic absorption studies[18–21] of transition-metal ions in various host semiconductor thin films and from crystal-field theory that the $^4T_1(P)$ energy level splits into four levels because of spin–orbit coupling. However, it is also known that Co^{2+} ions doped into ZnO can exhibit appreciable mixing between the $^4T_1(P)$ level and the higher-energy ^2G orbitals.

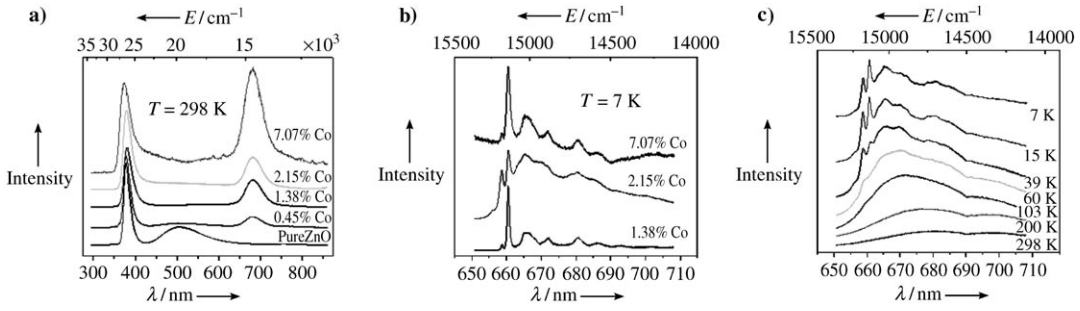

Figure 4. a) Room-temperature PL spectra of doped and undoped ZnO nanowires. The cobalt concentrations, as determined by EDX spectroscopy, are given above each spectrum. b) Low-temperature PL series of doped nanowires, which focus on the Co^{2+} ion transition ($^4T_1(P) \rightarrow {}^4A_2(F)$). c) Variable-temperature series of a sample of 2.15% Co-doped nanowires. All spectra have been vertically offset for clarity.

This orbital mixing complicates assignment of the PL peaks. In addition, other factors that must be considered are the surrounding Zn^{2+} ions, which can exert an additional anisotropic C_{3v} crystal-field potential on the dopant Co^{2+} ions, as well as the zero-field splitting parameter of the cobalt dopant. We consistently observed at least five peaks below 40 K in our low-temperature PL spectra. Their centers, from highest energy, are located at 15190, 15150, 15015, 14887, and 14700 m^{-1}. The fine structure is lost due to increased thermal energy above this temperature. We can relate these peaks to $^4T_1(P)$, $^2T_1(G)$, $^2E(G)\rightarrow$ground-state $^4A_2(F)$ internal Co^{2+} transitions based on previous reports.[20,21]

Finally, we examined the interaction of the cobalt dopant with the host ZnO semiconductor by electron paramagnetic resonance (EPR) spectroscopy. This technique has been used previously to characterize the environment of paramagnetic species in host lattices, such as $BaTiO_3$,[22,23] TiO_2,[24] and ZnO.[25,26] A series of EPR spectra at various temperatures is plotted in Figure 5a. A large resonance with a peak-to-peak

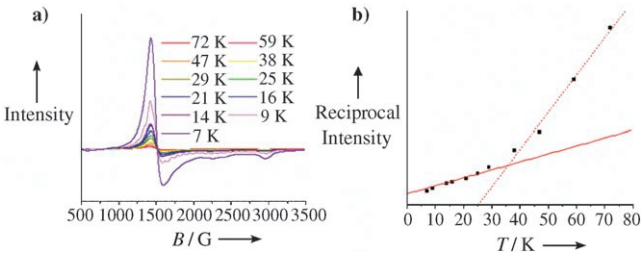

Figure 5. a) Temperature-dependent EPR spectra of $Zn_{1-x}Co_xO$ nanowires (Co = 2.15%). b) Reciprocal intensity versus temperature for the same sample. Intensities were obtained by numerical integration of the as-collected spectra twice. The solid line is a plot of the Curie Law, and the dashed line is fitted to the higher-temperature data points.

bandwidth of nearly 180 Gauss dominates the spectrum, with an additional smaller resonance that appears at higher field. The Landé g factors can be calculated as 4.43 and 2.23, which are assigned to $g_\perp$ and $g_\parallel$, respectively.[26] The reciprocal EPR intensity versus temperature for the sample of 2.15% Co is plotted in Figure 5b. The Curie Law predicts that this would be a straight line for isolated, paramagnetic Co^{2+} ions;[27] however, we observe a deviation from Curie behavior in the temperature region 25–30 K. The behavior is found in other nanowire samples with different cobalt concentrations as well. However, we are limited to measuring lightly doped nanowires by this method; nanowires with a cobalt concentration greater than 3% give very weak signals because of increased dipolar coupling between the cobalt centers.

This apparent deviation from normal paramagnetic behavior is interesting, particularly in light of various reports on the magnetic properties of this system. Indeed, many of those data, including our own and the studies cited herein, show magnetic behavior that cannot be modeled by a simple paramagnetic or ferromagnetic mechanism. It is a rather complex phenomenon, particularly considering the fact that detailed structural characterization indicates that transition-metal doping is homogenous and that there are no secondary phases present.

In summary, we have presented the synthesis of $Zn_{1-x}Co_xO$ nanowires from a solution-based synthetic route. Structural, optical, and spectroscopic characterizations indicate that the cobalt doping is substitutional for zinc cations in the host lattice. Although all signs suggest a completely uniform doping process, we note the existence of complex magnetic behavior that raises the possibility of multiple magnetic phases. Investigations are ongoing by us to elucidate the true nature of the observed magnetic behavior further.

Experimental Section

In a typical synthesis, zinc acetate (2.66 mmol) and cobalt(II) acetate (0.13 mmol, 0.05 equiv; a dopant concentration of 1.38 atom%) were mixed in a round-bottomed flask with trioctylamine (25 mL). The flask was fitted with a condenser and rapidly heated to 310 °C. The solids dissolved as the temperature increased, and the solution changed from clear to royal blue. The solution turned green after approximately 15–20 min, thus indicating the start of nanowire formation. The reaction was continued for 45–180 min depending on the length of wires desired and cooled to room temperature. The green precipitate was washed several times with ethanol to remove any cobalt precursor, as well as any cobalt metal particles. The green suspensions are stored in ethanol, and dilute solutions are stable for months. A typical synthesis yields approximately 60 mg of nanowires. The average cobalt concentration in the nanowires is typically 2–3% less than the amount added at the start of the reaction.

SEM images were taken on a JEOL-6340F field-emission scanning electron microscope operated at 5.0 kV. TEM images and EDX and EELS spectra were acquired on a Phillips CM200-FEG transmission electron microscope operated at 200 kV. Powder X-ray diffraction measurements were taken on a Bruker D-8 general area diffraction detection system. The X-ray source was $Co_{K\alpha}$ ($\lambda = 1.79$ Å).

PL measurements were performed on a single bundle of nanowires at each Co concentration by excitation with a He–Cd continuous wave laser emitted at 325 nm. A liquid-He-cooled cryostat was used for low-temperature PL measurements. EPR spectra were acquired on a Bruker EMX spectrometer operating at X-band (9.25 GHz) microwave frequency. The spectra were taken at a modulation amplitude of 2.5 Gauss and a microwave power of 10 mW. The g values were calculated from the resonance equation $h\nu = g\beta H_r$ (h is the Planck constant, ν is the microwave frequency, β is the Bohr magneton, and H_r is the resonant magnetic field).

Received: September 6, 2005
Published online: December 12, 2005

Keywords: doping · nanostructures · nanowires · semiconductors

[1] T. Dietl, H. Ohno, F. Matsukara, J. Cibert, D. Ferrand, *Science* **2000**, *287*, 1019.
[2] K. Sato, H. Katayama-Yoshida, *Phys. E* **2001**, *10*, 251.
[3] P. Sharma, A. Gupta, K. V. Rao, F. J. Owens, R. Sharma, R. Ahuja, J. M. O. Guillen, B. Johansson, G. A. Gehring, *Nat. Mater.* **2003**, *2*, 673.
[4] K. Ueda, H. Tabata, T. Kawai, *Appl. Phys. Lett.* **2001**, *79*, 988.
[5] D. C. Kundaliya, S. B. Ogale, S. E. Lofland, S. Dhar, C. J. Metting, S. R. Shinde, Z. Ma, B. Varughese, K. V. Ramanujachary, L. Salamanca-Riba, T. Venkatesan, *Nat. Mater.* **2004**, *3*, 709.

[6] J. H. Kim, H. Kim, D. Kim, Y. Ihm, W. K. Choo, *J. Eur. Ceram. Soc.* **2004**, *24*, 1847.
[7] J. H. Park, M. G. Kim, H. M. Jang, S. Ryu, Y. M. Kim, *Appl. Phys. Lett.* **2004**, *84*, 1338.
[8] S. Ramachandran, A. Tiwari, J. Narayan, *Appl. Phys. Lett.* **2004**, *84*, 5255.
[9] Y. Q. Chang, D. B. Wang, X. H. Luo, X. Y. Yu, X. H. Chen, L. Li, C. P. Chen, R. M. Wang, J. Xu, D. P. Yu, *Appl. Phys. Lett.* **2003**, *83*, 4020.
[10] J.-J. Wu, S.-C. Liu, M.-H. Wang, *Appl. Phys. Lett.* **2004**, *85*, 1027.
[11] L. Greene, M. Law, J. Goldberger, F. Kim, J. Johnson, Y. Zhang, R. Saykally, P. Yang, *Angew. Chem.* **2003**, *115*, 3139; *Angew. Chem. Int. Ed.* **2003**, *42*, 3031.
[12] L. Vayssieres, *Adv. Mater.* **2003**, *15*, 464.
[13] M. Yin, Y. Gu, I. L. Kuskovsky, T. Andelman, Y. Zhu, G. F. Neumark, S. O'Brien, *J. Am. Chem. Soc.* **2004**, *126*, 6206.
[14] D. A. Schwartz, N. S. Norberg, Q. P. Nguyen, J. M. Parker, D. R. Gamelin, *J. Am. Chem. Soc.* **2003**, *125*, 13205.
[15] D. A. Schwarz, K. R. Kittilstved, D. R. Gamelin, *Appl. Phys. Lett.* **2004**, *85*, 1395.
[16] Z. L. Wang, J. S. Yin, Y. D. Jiang, *Micron* **2000**, *31*, 571.
[17] D. H. Pearson, B. Fultz, C. C. Ahn, *Appl. Phys. Lett.* **1988**, *53*, 1405.
[18] H. A. Weakliem, *J. Chem. Phys.* **1962**, *36*, 2117.
[19] J. Ferguson, D. L. Wood, L. G. Van Uitert, *J. Chem. Phys.* **1969**, *51*, 2904.
[20] H.-J. Schulz, M. Thiede, *Phys. Rev. B* **1987**, *35*, 18.
[21] P. Koidl, *Phys. Rev. B* **1977**, *15*, 2493.
[22] E. Possenriede, P. Jacobs, O. F. Schrimer, *J. Phys. Condens. Matter* **1992**, *4*, 4719.
[23] R. N. Schwartz, B. A. Wechsler, *Phys. Rev. B* **1993**, *48*, 7057.
[24] B. Z. Rameev, F. Yildiz, L. R. Tagirov, B. Aktas, W. K. Park, J. S. Moodera, *J. Magn. Magn. Mater.* **2003**, *258*, 361.
[25] N. Jedrecy, H. J. von Bardeleben, Y. Zheng, J.-L. Cantin, *Phys. Rev. B* **2004**, *69*, 041308.
[26] M. Diaconu, H. Schmidt, A. Pöppl, R. Böttcher, J. Hoentsch, A. Klunker, D. Spemann, H. Hochmuth, M. Lorenz, M. Grunmann, *Phys. Rev. B* **2005**, *72*, 085214.
[27] J. E. Wertz, J. R. Bolton, *Electron Spin Resonance*, Chapman and Hall, New York, **1986**, p. 458.

